Proceedings of the IV Forum EMR–PL, June 27–29, 2016, Poznań, Poland

EPR Study of Dealuminated HY Zeolite and Silica Containing Cu–Mn–Zn Spinels: The Effect of Support

P. Decyk[a], A.B. Więckowski[b,c,*], L. Najder-Kozdrowska[b], I. Bilkova[a] and M. Ziółek[a]

[a]Adam Mickiewicz University, Faculty of Chemistry, Umultowska 89b, 61-614 Poznań, Poland

[b]University of Zielona Góra, Faculty of Physics and Astronomy, Institute of Physics, Z. Szafrana 4a, 65-516 Zielona Góra, Poland

[c]Institute of Molecular Physics, Polish Academy of Sciences, Division of Physics of Dielectrics and Molecular Spectroscopy, M. Smoluchowskiego 17, 60-179 Poznań, Poland

A mixture of antiferromagnetic $Cu_{1.4}Mn_{1.6}O_4$ and $Cu_{0.5}Zn_{0.5}Mn_2O_4$ or/and $ZnMn_2O_4$ spinels was prepared. Dealuminated HY zeolite and silica were doped by these Cu–Mn–Zn spinels. The materials were investigated by X-ray diffraction, the Fourier transform infrared spectroscopy and EPR spectroscopy. Additionally, all the samples were tested for their activity for isopropyl alcohol dehydration/dehydrogenation. Three EPR signals were observed for Cu–Mn–Zn/dealuminated HY and Cu–Mn–Zn/SiO_2 samples at 293 K. In contrast to the spectra recorded at 293 K, only one broad line attributed to Cu–Mn–Zn spinels was visible at 77 K. The EPR signal from pure Cu–Mn–Zn spinels consists only of a single broad line when recorded at 293 K, whereas at 77 K the line is narrower. For all samples subjected to evacuation at high vacuum up to 573 K, the Cu–Mn–Zn spinels were stable. The evacuation at 673 K resulted in a rapid lowering of the intensity of EPR spectrum.

DOI: 10.12693/APhysPolA.132.38

PACS/topics: 68.43.–h, 76.30.–v, 76.30.Fc, 82.75.Vx

1. Introduction

Catalysts based on copper–manganese mixed oxides are interesting materials for many catalytic processes. A large series of studies has been performed on the preparation of different Cu–Mn oxide systems, determination of their properties and their structure, as well as on the application of these systems as catalysts for various reactions. A special attention was paid to compounds with the general formula $Cu_xMn_{3-x}O_4$, having mostly the spinel structure. It is well-known that Cu and Mn cations in spinels exist in different valence states. The cations are distributed among two sublattices, one formed by the four-oxygen-coordinated tetrahedral A sites, and the other by the six-oxygen-coordinated octahedral B sites. It has been shown [1–4] that the A sites are occupied by Cu^+, Mn^{2+}, Mn^{3+} cations, and the B sites by Cu^{2+}, Mn^{3+}, Mn^{4+} cations. The octahedra occupied by Cu^{2+} or Mn^{3+} cations become elongated as a result of the Jahn–Teller effect.

The Cu–Mn mixed oxides show a high activity near room temperature for the oxidation of CO (e.g. hopcalite) [5–11] and the low temperature reduction of NO with NH_3 [12].

It has also been reported that Cu–Mn–Zn oxides supported on HY zeolite are active catalysts for dimethyl ether (DME) synthesis via direct CO hydrogenation [13, 14].

The interaction of metal ions in the above oxides and the role of a support used for these oxides as well as quantities of the latter present on the support are a very important question from the viewpoint of the aforementioned chemical processes. This is why attempts were made at solving the above question by applying various techniques: X-ray diffraction (XRD), ultraviolet and visible spectroscopy (UV-vis), infrared spectroscopy (IR), temperature-programmed desorption (TPD), temperature-programmed reduction (TPR), differential thermal analysis (DTA), thermogravimetric analysis (TG), however, only in a few studies devoted to this subject the EPR spectroscopy was employed [15–17]. The latter has been applied to investigations of spinels in NaY and HY zeolites which concerned interactions between Cu–Mn–Zn spinels and surfaces of the aforementioned zeolites [17]. The obtained results showed that the interactions strongly depend on the type of support. Therefore, we have undertaken research on physicochemical properties of Cu–Mn–Zn spinels-dealuminated HY zeolite and Cu–Mn–Zn spinels-amorphous silica systems. The aim of this study was to broaden the knowledge of the interactions between selected paramagnetic centers and the kind of support.

2. Experimental

2.1. Catalyst preparation

A commercial partially dealuminated NH_4Y zeolite (Si/Al = 4.2), Katalistiks b.v., was transformed into dealuminated HY by calcination in air at 673 K for 4 h. The dealuminated HY zeolite was mechanically mixed with 0.5, 1, 2, 5, 10, or 25 wt% of Cu–Mn–Zn component, which was synthesized according to the procedure described in Ref. [14]. After thorough crushing and grinding, the mixture was calcined in air at 723 K for 3 h. The same procedure was employed in the case of silica (VN3 Degussa).

*corresponding author; e-mail: Andrzej.Wieckowski@vp.pl

2.2. X-ray diffraction patterns

XRD patterns were recorded on a Bruker AXS D8 Advance X-ray diffractometer using Cu K_α radiation ($\lambda = 0.154$ nm) in the step scanning mode of 0.05° in the 2Θ range between 10° and 60°.

2.3. Fourier transform infrared (FTIR) spectra

The FTIR spectra were recorded on a Vector 22 (Bruker) spectrometer. The pellets of dealuminated HY zeolite for structural examinations were prepared using a zeolite sample and KBr (1 mg and 200 mg, respectively) followed by compressing the mixture.

Surface properties of dealuminated HY zeolite were studied by *in situ* FTIR spectroscopy of adsorbed pyridine. Self-supporting pellet of about 10 mg/cm^2 was prepared and placed into a glass cell connected to a vacuum line. FTIR spectra were recorded at 293 K. The dealuminated HY sample was activated at 673 K under vacuum before any performing characterization. Pyridine vapor was adsorbed at 373 K followed by evacuation at various temperatures (373–673 K) for 30 min at each temperature. The FTIR spectrum of the sample was subtracted from that recorded after pyridine adsorption.

2.4. Catalytic dehydration/dehydrogenation of isopropanol

FTIR studies were complemented by performing catalytic dehydration/dehydrogenation of isopropanol (Chempur, Poland) in an on-line pulse reactor made of glass, connected to a gas chromatograph CHROM-5. Granulated samples of 0.05 g were activated at 673 K for 2 h under helium flow (40 cm^3/min). Isopropanol conversion was measured in the temperature range of 423–573 K. The injected volume of the alcohol was 3 μL. The post-reaction mixture (products and unreacted part of 2-propanol) was separated on a 2 m column packed with Carbowax 400 on Chromosorb W (80–100 mesh) at 363 K in a helium flow of 40 cm^3/min. A thermal conductivity detector (TCD) has been used in the chromatographic measurements.

2.5. EPR measurements

The EPR measurements of powder samples were carried out using an X-band EPR spectrometer type SE/X 2547 RADIOPAN. The operating microwave frequency was in the range of 8.9 GHz with a magnetic field modulation of 100 kHz. The spectra were recorded at room temperature (293 K) and at liquid nitrogen temperature (77 K) for all the samples studied.

For all untreated dealuminated HY samples with loadings from 0.5 to 25 wt%, the EPR spectra were taken at 77 K and 293 K, whereas in the case of dealuminated HY zeolite with the loading of 10 wt% the EPR spectra were measured in the temperature range of 77–403 K. Additionally, the samples of dealuminated HY zeolite and silica with 10 wt% loading were evacuated in a high vacuum of 10^{-4} Torr in the temperature range of 293–673 K. The evacuation time at 293 K was 6 h, while at higher temperatures it was 2 h. The EPR spectra were recorded at 293 K and 77 K.

3. Results and discussion

3.1. XRD results

The XRD patterns of pure Cu–Mn–Zn spinels as well as those of dealuminated HY zeolite and silica modified by these spinels are shown in Fig. 1. A comparison of the obtained XRD profiles with those found in the database JCPDS-International Centre for Diffraction Data has permitted to assign the two reflections to $Cu_{1.4}Mn_{1.6}O_4$ and $Cu_{0.5}Zn_{0.5}Mn_2O_4$ or/and $ZnMn_2O_4$. The spinel $Cu_{1.4}Mn_{1.6}O_4$ (the first reflection labeled as 1) at $2\theta = 35.7°$ has a cubic symmetry and the space group $Fd\text{-}3m(227)$ with the lattice constant $a = 8.305$ Å (PDF Card number 01-071-1145). The second reflection (labeled as 2) at $2\theta = 36.4°$ can be attributed to the spinels $ZnMn_2O_4$ (hetaerolite) or/and $Cu_{0.5}Zn_{0.5}Mn_2O_4$. They have tetragonal symmetry with space group $I41/amd(141)$ (PDF Card number 04-005-7644 and 04-007-4373). Unfortunately, in this case a direct distinction between zinc and copper-zinc manganite is very difficult because the lattice parameters have nearly identical values: $a = 5.73$ Å, $c = 9.25$ Å and $a = 5.72$ Å, $c = 9.23$ Å, respectively. The intensities of diffraction peaks for zinc and copper–zinc manganite spinels are smaller than for copper manganite. This can indicate that the zinc and copper–zinc manganite spinels are present in smaller amounts. It is worthy to notice that XRD patterns as well as FTIR spectra recorded in the range of 400–1500 cm^{-1} have confirmed that the crystal structure of dealuminated HY zeolite was preserved after the deposition of Cu–Mn–Zn spinels.

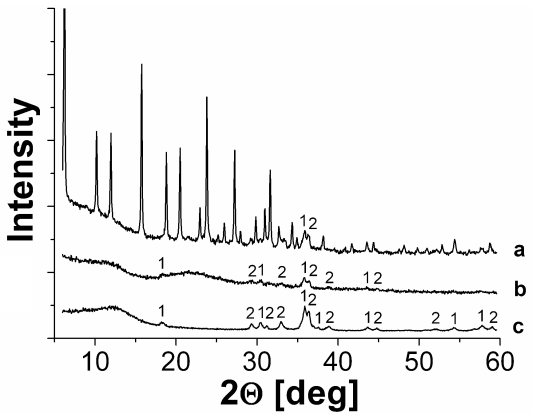

Fig. 1. XRD patterns of Cu–Mn–Zn spinels loaded onto dealuminated HY zeolite (10 wt%) (a), silica (10 wt%) (b) and Cu–Mn–Zn spinels (c). 1 — $Cu_{1.4}Mn_{1.6}O_4$, 2 — $Cu_{0.5}Zn_{0.5}Mn_2O_4/ZnMn_2O_4$.

3.2. Surface properties

3.2.1. FTIR studies of adsorbed pyridine

To identify the type of sites on the surface of dealuminated HY zeolite we have employed pyridine (Py) as a probe molecule which was adsorbed on the zeolite surface, followed by evacuation in the temperature range from 473 K to 673 K. The FTIR spectra of evacuated dea-

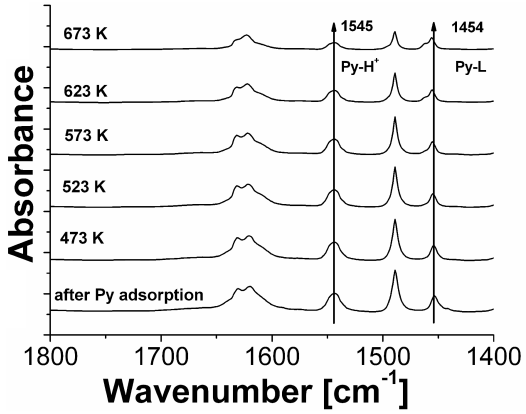

Fig. 2. FTIR spectra after pyridine adsorption on dealuminated HY zeolite, followed by desorption *in vacuo* at different temperatures.

luminated HY sample are presented in Fig. 2. The spectra of the samples subjected to pyridine adsorption and evacuation at 473 K revealed the presence of two kinds of acid centers: Brønsted acid sites (BAS) estimated by the band at ≈ 1545 cm^{-1} typical of vibrations of pyridinium cations and Lewis acid sites (LAS) that give rise to the band at ≈ 1454 cm^{-1} assigned to vibrations of coordinatively bonded pyridine [18]. The band at 1454 cm^{-1} originating from pyridine chemisorbed on Lewis acid sites (LAS) remains unchanged even after evacuation at 673 K. On the other hand, BAS react with pyridine to form pyridinium cations (PyH^+) that are responsible for the presence of the IR band at ≈ 1545 cm^{-1}. However, in the contrast to LAS, intensities of this band decline after evacuation at 623 K. This indicates that LAS on dealuminated HY zeolite are stronger than BAS.

3.2.2. Isopropanol dehydration/dehydrogenation

FTIR studies of surface acidity of dealuminated HY zeolite were supplemented by measurements of catalytic activity for isopropanol dehydration/dehydrogenation on pure Cu–Mn–Zn spinels, as well as on dealuminated HY zeolite and silica modified by these spinels. Isopropyl alcohol undergoes dehydration to propene and/or diisopropyl ether on acidic sites and dehydrogenation to acetone on basic and redox centers [19–22].

TABLE I

Catalytic activity and selectivity for dehydration/dehydrogenation of isopropanol at 523 K to: propene (A), diisopropyl ether (B) and acetone (C). Average results from the 2nd and 3rd pulse.

Catalyst	Isopropanol conversion [%]	Selectivity [%] to		
		A	B	C
HY	100	100	0	0
Cu–Mn–Zn/dealuminated HY (10 wt%)	100	100	0	0
Cu–Mn–Zn/SiO_2 (10 wt%)	41	7.0	0.2	92.8
Cu–Mn–Zn spinels	18	2.8	0	97.2

The results of the catalytic measurements are presented in Table I. The both materials, dealuminated HY and Cu–Mn–Zn/dealuminated HY (10 wt%), are characterized by a high degree of isopropanol conversion which reaches 100% in the whole temperature range studied. The main product of dehydration/dehydrogenation was propene produced with the selectivity of 100%, except for Cu–Mn–Zn/dealuminated HY (10 wt%), where besides propene, also diisopropyl ether was formed. Such a situation was observed only at 423 K, whereas at higher temperatures only propene was produced. On the other hand, pure spinels and silica-supported spinels (10 wt%) have demonstrated markedly different acid-base properties. The above materials began to be catalytically active at 523 K and for this reason the latter temperature has been chosen for comparing activity and selectivity of all investigated samples. One can notice that in the case of Cu–Mn–Zn/dealuminated HY (10 wt%) the predominant influence on the catalytic behavior comes from the dealuminated HY component, whereas in that of Cu–Mn–Zn/SiO_2, the Cu–Mn–Zn spinels determine catalytic properties, as evidenced by over 90% selectivity to acetone observed for Cu–Mn–Zn/SiO_2 (10 wt%) and Cu–Mn–Zn spinels.

3.3. EPR results

For all untreated samples of dealuminated HY zeolites, irrespective of loading, three types of lines were observed in the EPR spectra recorded at 293 K (Fig. 3a). The first line is broad and originates from spinels present on the surface of the zeolite. The second one is anisotropic and can be attributed to four-component hyperfine structure (hfs) from isolated Cu^{2+} cations ($S = 1/2$, ^{63}Cu, ^{65}Cu, $I = 3/2$ both). The third signal, that is an isotropic line, comes from the six-component hfs of isolated Mn^{2+} cations ($S = 1/2$, ^{55}Mn, $I = 5/2$). The second and third signal originate from solid-state ion-exchange of Cu^{2+} and Mn^{2+} cations (in spinels) with H^+ (BAS) of dea-

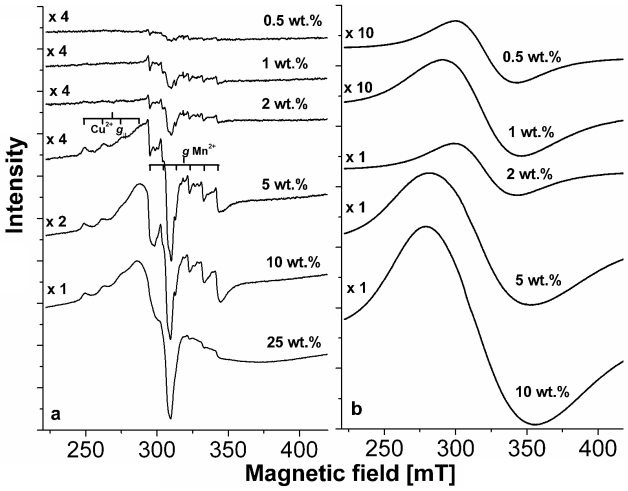

Fig. 3. EPR spectra of dealuminated HY zeolite with different loading of Cu–Mn–Zn spinels, recorded at 293 K (a) and 77 K (b).

luminated HY zeolite [23]. With the increase in the concentration of the spinel phase, individual hfs lines from Cu^{2+} and Mn^{2+} undergo broadening due to spin–spin interactions which result in the reduction in the resolution of spectra measured at 293 K. For all samples, regardless of spinel loading, the spectra recorded at 77 K have shown only a single nearly symmetric EPR line (Fig. 3b). The resonance field B_{res} did not change significantly with rising concentration of the spinels in dealuminated HY zeolite, however, the linewidth ΔB_{pp} increased (Table II).

TABLE II

Values of resonance fields B_{res} (± 2, [mT]) and linewidths ΔB_{pp} (± 2, [mT]) for dealuminated HY zeolite with different loadings [wt%] of Cu–Mn–Zn spinels, recorded at 77 K.

Loading	B_{res}	ΔB_{pp}
0.5	322	42
1	319	54
2	321	44
5	318	70
10	318	76

TABLE III

Parameters of EPR spectra (g-factors [–], hyperfine splittings a [mT]) for samples containing Cu–Mn–Zn spinels loaded onto different supports (untreated samples, 293 K).

Complex:		Cu (I)			Cu (II)			Mn	
Support	Load [%]	$g_\parallel$ ± 0.005	$a_\parallel$ ± 0.1	$g_\perp$ ± 0.005	$g_\parallel$ ± 0.005	$a_\parallel$ ± 0.1	$g_\perp$ ± 0.005	g 0.001	a ± 0.1
NaY [17]	10	2.355	12.3	2.055	–	–	–	–	–
HY [17]	5	2.373	12.4	2.067	2.331	15.7	2.038	2.002	9.5
	1	2.373	12.5	2.065	2.331	15.6	2.037	2.001	9.6
dealuminated HY	0.5	–	–	–	–	–	–	2.001	9.5
	1	–	–	2.068	–	–	–	2.001	9.5
	2	2.374	12.6	2.068	–	–	–	2.002	9.5
	5	2.370	12.6	2.066	–	–	–	2.001	9.5
	10	2.377	13.2	2.070	–	–	–	2.000	9.5
	25	2.366	12.9	2.066	–	–	–	–	9.9
SiO_2	10	–	–	2.062	–	–	–	–	–

The spin-Hamiltonian parameters of EPR spectra, $g_\parallel$, $g_\perp$, $a_\parallel$, for Cu^{2+} complex in the samples containing Cu–Mn–Zn spinels supported on dealuminated HY zeolite (untreated samples), recorded at 293 K, are given in Table III. The hyperfine structure (hfs) lines at the perpendicular orientation were poorly resolved and therefore the value of $a_\perp$ could not be determined.

In Table III there are also shown the spin Hamiltonian parameters of two Cu^{2+} complexes observed in the EPR spectra of Cu–Mn–Zn spinels supported on non-dealuminated HY zeolite [17]. Contrary to non-dealuminated HY, only one type of Cu^{2+} complex was observed in dealuminated HY and NaY zeolites [17]. The values of the spin-Hamiltonian parameters shown for Cu^{2+} complex I prove that the inequality $g_\parallel > g_\perp > g_e = 2.0023$ is fulfilled. Therefore the orbital ground state of the unpaired electron of Cu^{2+} complex is $|x^2 - y^2\rangle$. Taking into account the Jahn–Teller effect, one can conclude

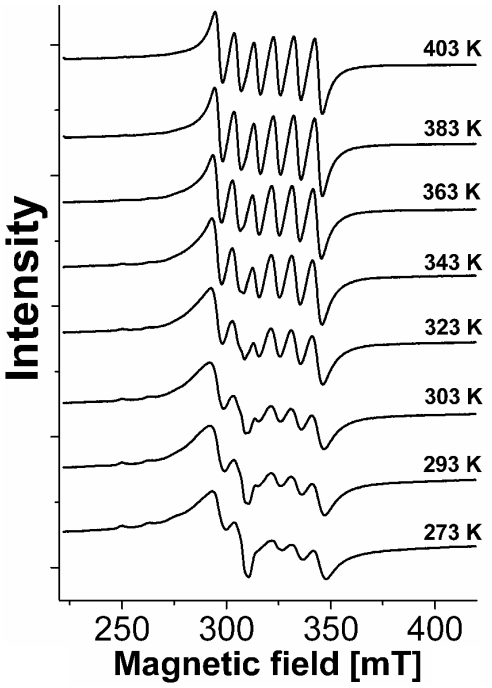

Fig. 4. Changes in EPR spectra with temperature for dealuminated HY zeolite containing Cu–Mn–Zn spinels (10 wt%).

that the Cu^{2+} complex I has the symmetry of tetragonally elongated *trans*-octahedron D_{4h} [24].

The EPR spectrum of Mn^{2+} complex in dealuminated HY zeolite shows six hfs lines originating from the $m_s|-1/2\rangle \rightarrow |+1/2\rangle$ transition (see Fig. 3a). Between the six hfs lines we have observed additional peaks (Fig. 3a) which resulted from the forbidden transitions [25] caused by the zero-field splitting (zfs) [26]. The forbidden transitions were also seen for non-dealuminated sample of Cu–Mn–Zn/HY (10 wt%) [17]. The linewidth of individual hfs lines of Mn^{2+} complexes decreases with increasing temperature as illustrated in Fig. 4. This indicates the role of dynamic processes, e.g. random tumbling, occurring in the Mn^{2+} complexes.

It is worth noting that for Cu–Mn–Zn spinels on silica (10 wt%), the EPR spectrum recorded at 293 K is very weak. Only the strongest part of the powder spectrum for perpendicular orientation of Cu^{2+} cation at $g_\perp = 2.062$ (Table III) has been observed. The absence of resolved lines of Cu^{2+} and Mn^{2+} complexes is a result of surface properties of silica. Contrary to dealuminated HY zeolite, pure silica has a low concentration of BAS and isolated Cu^{2+} and Mn^{2+} complexes are present in a small amount. However, EPR spectrum of this sample recorded at 77 K shows a strong broad line derived from antiferromagnetic spinels $Cu_{1.4}Mn_{1.6}O_4$ and $Cu_{0.5}Zn_{0.5}Mn_2O_4$ or/and $ZnMn_2O_4$.

In Table IV the values of linewidths ΔB_{pp} for some of the studied samples are given. It can be seen that at 77 K a lowering of the linewidth takes place. This effect was more visible when silica was the support.

TABLE IV

Values of linewidth ΔB_{pp} (±2 [mT]) for materials studied at 293 K and 77 K.

Catalyst	293 K	77 K
Cu–Mn–Zn spinels	104	89
Cu–Mn–Zn/dealuminated HY (10 wt%)	–	76
Cu–Mn–Zn/SiO_2 (10 wt%)	108	45

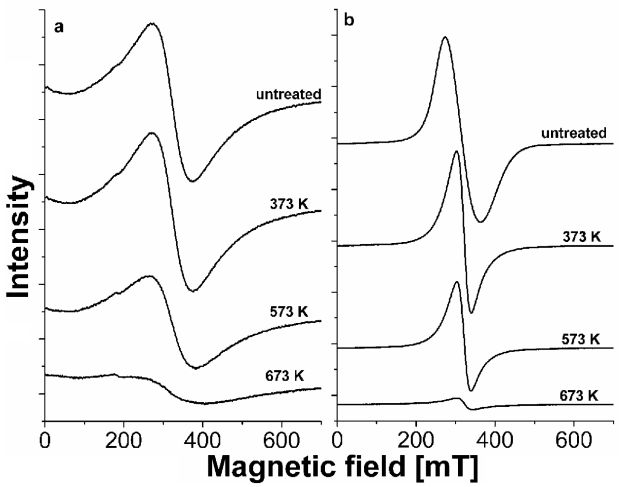

Fig. 5. EPR spectra of Cu–Mn–Zn spinels evacuated at different temperatures. Spectra recorded at 293 K (a) and 77 K (b).

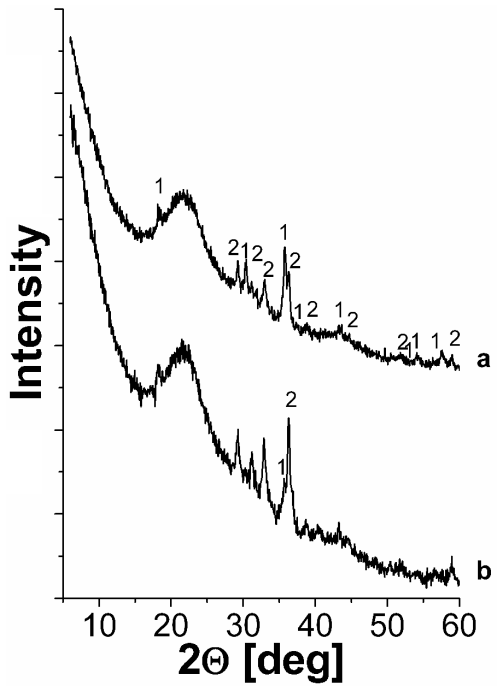

Fig. 6. XRD patterns of Cu–Mn–Zn spinels for untreated sample (a) and after evacuation at 673 K (b). 1 — $Cu_{1.4}Mn_{1.6}O_4$, 2 — $Cu_{0.5}Zn_{0.5}Mn_2O_4/ZnMn_2O_4$.

The Cu–Mn–Zn spinels were evacuated at different temperatures. The EPR spectra of the above material after evacuation are shown in Fig. 5. The spectra (a) were recorded at 293 K and the spectra (b) at 77 K. The high vacuum treatment at 673 K resulted in a sudden lowering of EPR line intensity which indicates the occurrence of transformations of the mixture of Cu–Mn–Zn spinels. This phenomenon was confirmed by XRD patterns shown in Fig. 6.

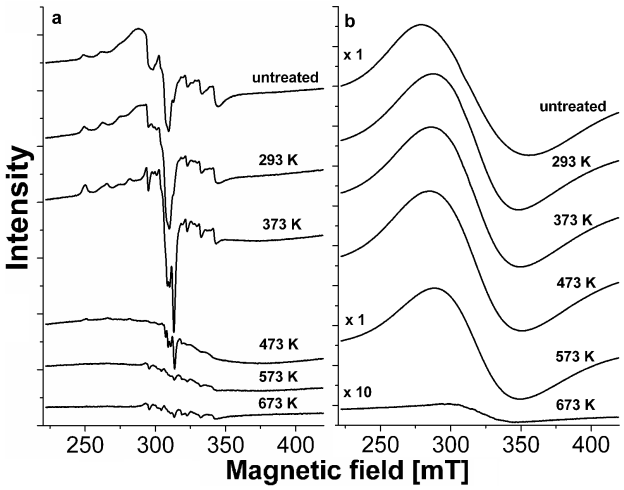

Fig. 7. EPR spectra of dealuminated HY zeolite containing Cu–Mn–Zn spinels (10 wt%), evacuated at different temperatures. Spectra recorded at 293 K (a) and 77 K (b).

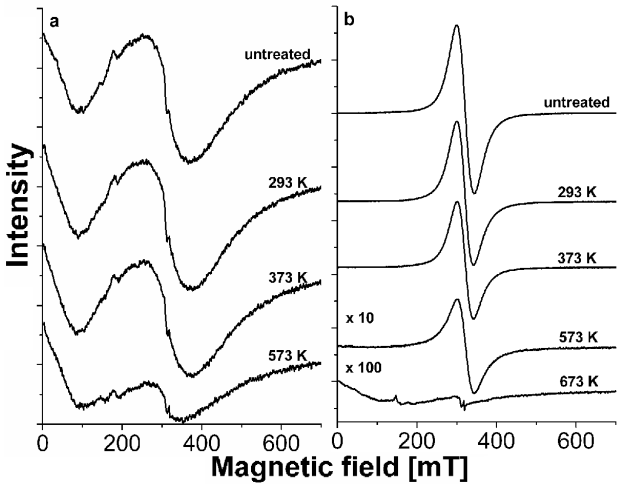

Fig. 8. EPR spectra of SiO_2 containing Cu–Mn–Zn spinels (10 wt.%), evacuated at different temperatures. Spectra recorded at 293 K (a) and 77 K (b).

The dealuminated HY zeolite containing Cu–Mn–Zn spinels (10 wt%) was also subjected to evacuation at different temperatures. The EPR spectra of this sample (after evacuation) are presented in Fig. 7. The spectra recorded at 293 K (a) differ from those recorded at 77 K (b). The EPR spectra of Cu–Mn–Zn/dealuminated HY (10 wt%) recorded at 293 K, after the evacuation at

473 K and at higher temperatures, are characterized by considerably reduced intensities of EPR lines originated from Cu^{2+} and Mn^{2+} cations. The evacuation at higher temperatures led to lowering of valence states of cations which are EPR silent.

It is worth noting that EPR spectra of Cu–Mn–Zn/dealuminated HY (10 wt%), recorded at 77 K, do not show significant changes in the line shape and line intensity, when the above material was evacuated up to 573 K. Only after the evacuation at 673 K a great reduction occurred in the signal intensity. This can be a result of the transformation that took place in the spinels deposited on dealuminated HY zeolite, which was confirmed for pure Cu–Mn–Zn spinels.

Similarly to Cu–Mn–Zn/dealuminated HY (10 wt%), the evacuation of Cu–Mn–Zn/SiO_2 (10 wt%) at 673 K resulted in a considerable reduction in the EPR signal (Fig. 8). This effect is better visible for the spectra recorded at 77 K because in the case of the spectra recorded at 293 K the intensities of EPR signals are weaker.

4. Conclusions

The EPR line for Cu–Mn–Zn spinels ($Cu_{1.4}Mn_{1.6}O_4$ and $Cu_{0.5}Zn_{0.5}Mn_2O_4$ or/and $ZnMn_2O_4$) is broad at 293 K and narrower at 77 K.

The kind of support (dealuminated HY zeolite or silica) determines the character of the EPR spectrum recorded at 293 K.

In the case of dealuminated HY zeolites containing Cu–Mn–Zn spinels a broad line from Cu–Mn–Zn spinels and lines derived from Cu^{2+} and Mn^{2+} complexes were observed in the EPR spectra. The presence of Cu^{2+} and Mn^{2+} complexes could be observed in the EPR spectra only at 293 K and higher temperatures. At liquid nitrogen temperature (77 K), only a broad line from Cu–Mn–Zn spinels was detected. The Cu^{2+} and Mn^{2+} complexes originate from the solid state ion exchange and are located in extra-lattice positions. The temperature dependence of the linewidth of individual hfs lines for Mn^{2+} cations indicates the occurrence of dynamic processes proceeding in the zeolite lattice.

In contrast to dealuminated HY zeolite, the solid state ion exchange in silica-based samples is poor because of weak acidity of their BAS. The EPR spectra recorded at 293 K show only a broad line from Cu–Mn–Zn spinels and a very weak signal from isolated Cu^{2+} cations.

The evacuation (at 673 K, in high vacuum conditions) of pure spinels and spinels supported on dealuminated HY zeolite and silica resulted in the disappearance of EPR line originated from Cu–Mn–Zn spinels in the spectra recorded at 77 K. The evacuation brought about a great reduction in EPR line intensity which indicates that Cu–Mn–Zn spinels underwent transformations.

Acknowledgments

The authors are grateful to Professor Ryszard Fiedorow (Adam Mickiewicz University, Poznań, Poland) for helpful discussions.

References

[1] R.E. Vandenberghe, G.G. Robbrecht, V.A.M. Brabers, *Mater. Res. Bull.* **8**, 571 (1973).

[2] A.D.D. Broemme, V.A.M. Brabers, *Solid State Ion.* **16**, 171 (1985).

[3] B. Gillot, S. Buguet, E. Kester, *J. Mater. Chem.* **7**, 2513 (1997).

[4] P. Wei, M. Bieringer, L.M.D. Cranswick, A. Petric, *J. Mater. Sci.* **45**, 1056 (2010).

[5] F.S. Stone, *Adv. Catal.* **13**, 1 (1962).

[6] G.M. Schwab, S.B. Kanungo, *Z. Phys. Chem. Neue Fol.* **107**, 109 (1977).

[7] S. Vepřek, D.L. Cocke, S. Kehl, H.R. Oswald, *J. Catal.* **100**, 250 (1986).

[8] L.S. Puckhaber, H. Cheung, D.L. Cocke, A. Clearfield, *Solid State Ion.* **32-33**, 206 (1989).

[9] I. Spassova, D. Mehandjiev, *React. Kinet. Catal. Lett.* **58**, 57 (1996).

[10] G.J. Hutchings, A.A. Mirzaei, R.W. Joyner, M.R.H. Siddiqui, S.H. Taylor, *Appl. Catal. A Gen.* **166**, 143 (1998).

[11] F.C. Buciuman, F. Patcas, T. Hahn, *Chem. Eng. Process.* **38**, 563 (1999).

[12] M. Kang, E.D. Park, J.M. Kim, J.E. Yie, *Catal. Today* **111**, 236 (2006).

[13] J.H. Fei, M.X. Yang, Z.Y. Hou, X.M. Zheng, *Energ. Fuel.* **18**, 1584 (2004).

[14] J.H. Fei, Z.Y. Hou, B. Zhu, H. Lou, X.M. Zheng, *Appl. Catal. A Gen.* **304**, 49 (2006).

[15] A.K. Bandyopadhyay, *J. Mater. Sci.* **15**, 1605 (1980).

[16] T.H. Bennur, D. Srinivas, P. Ratnasamy, *Microp. Mesopor. Mater.* **48**, 111 (2001).

[17] P. Decyk, A.B. Więckowski, L. Najder-Kozdrowska, I. Bilkova, *Nukleonika* **60**, 423 (2015).

[18] H.G. Karge, M. Hunger, H.K. Beyer, in: *Catalysis and Zeolites: Fundamentals and Applications*, Eds. J. Weitkamp, L. Puppe, Springer, Berlin 1999, p. 198.

[19] P.A. Jacobs, M. Tielen, J.B. Uytterhoeven, *J. Catal.* **50**, 98 (1977).

[20] P.A. Jacobs, J.B. Uytterhoeven, *J. Catal.* **50**, 109 (1977).

[21] P.E. Hathaway, M.E. Davis, *J. Catal.* **119**, 497 (1989).

[22] C. Lahousse, J. Bachelier, J.C. Lavalley, H. Lauron-Pernot, A.M. Le Govic, *J. Mol. Catal.* **87**, 329 (1994).

[23] Zh. Li, K. Xie, R.C.T. Slade, *Appl. Catal. A Gen.* **209**, 107 (2001).

[24] J. Goslar, A.B. Więckowski, *J. Solid State Chem.* **56**, 101 (1985).

[25] B. Bleaney, R.S. Rubins, *Proc. Phys. Soc.* **77**, 103 (1961).

[26] Z. Olender, D. Goldfarb, J. Batista, *J. Am. Chem. Soc.* **115**, 1106 (1993).